Direct measurements of blood glucose concentration in the presence of saccharide interferences using slope and bias orthogonal signal correction and Fourier transform near-infrared spectroscopy

David Abookasis[a,*] and Jerome J. Workman[b,c]
[a]Ariel University Center of Samaria, Department of Electrical and Electronics Engineering, Ariel 44837, Israel
[b]Biotechnology Business Associates, Orange County, California 92612
[c]Liberty University, Lynchburg, Virginia 24502

Abstract. Saccharide interferences such as Dextran, Galactose, etc. have a great potential to interfere with near infrared (NIR) glucose analysis since they have a similar spectroscopic fingerprint and are present physiologically at large relative concentrations. These can lead to grossly inappropriate interpretation of patient glucose levels and resultant treatment in critical care and hospital settings. This study describes a methodology to reduce this effect on glucose analysis using an NIR Fourier transform spectroscopy method combined with a multivariate calibration technique (PLS) using preprocessing by orthogonal signal correction (OSC). A mathematical approach based on the use of a single calibration based bias and slope correction was applied in addition to a standard OSC was investigated. This approach is combined with a factorial interferent calibration design to accommodate for interference effects. We named this approach as a slope and bias OSC (*sb*OSC). *sb*OSC differs from OSC in the way it handles the prediction. In *sb*OSC, statistics on slope and bias obtained from a set of calibration samples are then used as a validation parameter in the prediction set. Healthy human volunteer blood with different glucose (80 to 200 mg/dL) and hematocrit (24 to 48 vol.%) levels containing high expected levels of inteferents have been measured with a transmittance near-infrared Fourier transform spectrometer operates in the broadband spectral range of 1.25–2.5 μm (4000–8000 cm^{-1}). The effect of six interferents compounds used in intensive care and operating rooms, namely Dextran, Fructose, Galactose, Maltose, Mannitol, and Xylose, were tested on blood glucose. A maximum interference effect (MIE) parameter was used to rank the significance for the individual interferent type on measurement error relative to the total NIR whole blood glucose measurement error. For comparison, a YSI (Yellow Springs Instrument) laboratory reference glucose analyzer and NIR data were collected at the same time as paired samples. MIE results obtained by *sb*OSC were compared with several standard spectral preprocessing approaches and show a substantial reduced effect of saccharide interferences. NIR glucose measurement results are substantially improved when comparing standard error of prediction from validation samples; and resulting MIE values are small. [DOI: 10.1117/1.3540408]

Keywords: orthogonal signal correction; fourier transform infrared spectroscopy; blood glucose measurements; saccharide interferents; maximum interference effect.

Paper 10305RR received Jun. 2, 2010; revised manuscript received Dec. 14, 2010; accepted for publication Dec. 21, 2010; published online Feb. 10, 2011.

1 Introduction

Monitoring and quantification of glucose level in blood is an important ongoing field of research in clinical analysis.[1,2] Specifically, monitoring blood glucose by near infrared spectroscopy (NIRS) has become one of the most active areas in biomedical optics and pharmaceutical research investigated over 20 years by many research groups.[3–6] More recently, interest in NIRS is on the rise for strict continuous control of blood glucose levels for patients in an intensive care unit (ICU) and operating room (OR) known as tight glycemic control (TGC).[7] In TGC, blood glucose is frequently (four to six daily measurements) or continuously monitored in order to provide information needed to administer the proper amount of insulin or glucose in order to avoid hypoglycemia or hyperglycemia while maintaining normoglycemia (80 to 110 mg/dL).[8] Recently, Tang et al. report on the effect of 30 drugs used in hospitals on glucose measurement with handheld glucose meters and a portable glucose analyzer.[9] To date, however, very little research is available describing the influence of drugs, found in many patients while treated in ICU, on NIRS measurements. The Food and Drug Administration of the United States also requires understanding regarding the effect of drugs on accuracy and precision for blood glucose assays using NIRS. In general, the measurement of blood glucose by any technique is inherently complex because of the wide range of potentially interfering components in blood and body tissues. Therefore, a study designed to screen the influence of interferent substances at clinically relevant concentrations is necessary.

The clinical and laboratory standards institute (CLSI) refer to the term interference as a cause of clinically significant

Address all correspondence to: David Abookasis, Ariel University, Center of Samaria, Department of Electrical and Electronics Engineering, Ariel 44837, Israel. E-mail: davida@ariel.ac.il.

1083-3668/2011/16(2)/027001/9/$25.00 © 2011 SPIE

bias in the measured analyte concentration due to the effect of another component or property of the sample.[10] By clinical significance we mean the importance of an error to its potential to alter a physician's diagnosis, treatment, or management of a patient. One of our goals in this study was to evaluate the effects of test interferent compounds on NIRS glucose prediction errors. The main test interferences for this evaluation are saccharide compounds, suspected as having the greatest potential to interfere with NIR glucose analysis. Saccharide compounds can be divided into three main groups: 1. monosaccharides (e.g., fructose, galactose, mannitol, and xylose), 2. disaccharides (e.g., maltose), and 3. polysaccharides (e.g., dextran and hetastarch). These saccharides are suspect since they have similar spectroscopic fingerprints to glucose and may be present physiologically at large relative concentrations. The selection of specific interferents and test concentration levels for interference testing are gathered from a variety of reference literature sources. Although not comprehensive in these literature, sources for interference information include the following: common handheld meter interferences, selected interferences from the EP7-A2 guidelines (high concentrations), and commonly used drugs in ICUs.

To reduce or eliminate the effect of these saccharide compounds on glucose measurements, a preprocessing method such as orthogonal signal correction (OSC) can be used. OSC aims to remove strong structured variation from the spectral data, $\boldsymbol{X}$, that is unrelated, or orthogonal, to the concentration $\boldsymbol{Y}$.[11] To achieve such orthogonality, $\boldsymbol{X}$ is decomposed into scores (t), which are required to be orthogonal to $\boldsymbol{Y}$, and loading (p) vectors. Multivariate calibration by partial least squares (PLS) is accomplished with $\boldsymbol{X}$ calibrated against scores and new scores and loadings are recalculated.[12] Next, new scores and loadings, which contain information not related to the concentration, are subtracted from $\boldsymbol{X}$ in order to correct the spectra. For new spectral data, $\boldsymbol{X_{new}}$, a new score vector is calculated and multiplied with the transpose of the loading vector previously found. Finally, the product of the two is subtracted from $\boldsymbol{X_{new}}$. This type of mathematical treatment has been applied here with one more element; during calibration and validation modeling the bias (intercept) and slope from the prediction data sets, that are not included in the calibration model, were determined. This process was repeated 100 times (~10% of the model size across the entire set) in order to compute statistic power on the bias and slope parameter. For each new validation spectra, both the prediction vector, $\hat{b}$, and the bias and slope from the calibration process were automatically applied yielding a standardized prediction. A flow chart describing the difference between OSC and slope and bias OSC (*sb*OSC) is depicted in Fig. 1.

In this work, the ability to determine glucose concentration in the presence of saccharide interferences in NIRS measurements by using Fourier transform near-infrared spectroscopy (FT-NIRS) with a modification to OSC, for the first time to our knowledge, was investigated. Detailed results demonstrate the use of a single calibration for quantitative determination of glucose levels in whole blood samples from 14 healthy anonymous patients. These patient samples contained maximum physiological levels of six different saccharides. The measurement error effect of the individual interferents was determined based on the maximum interference effect (MIE) of each substance. Furthermore, the detailed use of FT-NIRS in transmission mode coupled with *sb*OSC and a single PLS calibration model for determination of glucose in whole blood will be described.

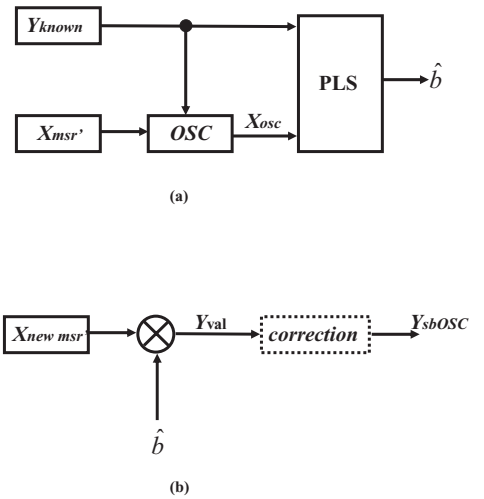

Fig. 1 Flow chart describing the difference between OSC procedures to *sb*OSC. (a) Calibration, (b) Validation. *sb*OSC contribution achieved on the validation side.

2 Material and Methods

2.1 *Instrumentation*

The transmittance Fourier transform near-infrared (FT-NIR) spectrometer was designed and built in-house that has an operating wavelength range of 1.25–2.5 μm (4000–8000 cm^{-1}) with a spectral resolution of 32 cm^{-1}. It uses the same basic optical configuration of a Michelson interferometer platform.[13] The spectrometer consists of a uniform, constant, blackbody light source (mini-igniter) with a color temperature of approximately 1035 °C, matched fused silica beam splitter and compensator plates, fixed and moveable (active) corner-cube retroreflectors, 1 mm diameter extended-wavelength InGaAs PIN photodiode, and a data acquisition system that digitizes the interferogram data and stores them on PC. The interferogram data was processed and analyzed off-line using MatLab. Light reaching the sample is high pass filtered by the use of a silicon collimator lens that attenuates wavelengths below 1.05 μm. A spring suspension system along with a voice coil actuator is used to move the active retroreflector in a strictly axial direction. The active mirror is continuously scanning at a constant velocity of 0.8 $cm \cdot s^{-1}$, 70% duty cycle, which results in approximately eight interferograms per second. The blood and background (Saline) samples were pumped through a borosilicate flow cell with a path length of 1 mm that was controlled at 34 °C.

2.2 *Sample Handling*

Human blood was collected from healthy human donors in the morning between 7:30 to 9:00 am on each testing day. Using a venipuncture technique, blood is drawn into multiple 50 mL heparinized syringes. Blood is immediately transported to our lab by motor vehicle, which takes approximately 30 min. Once at the lab, blood syringes are transferred to 50 mL centrifuge tubes. A small and well-mixed sample is used for native hematocrit (Hct)

and glucose readings. A VWR clinical 200 large centrifuge with Hct adapter and YSI 2300 glucose analyzers are respectively utilized to measure Hct and glucose values. Regardless of Hct volume percentage, all blood tubes are spun down at 3000 rpm for 5 min using the VWR centrifuge with 50 mL tube adapter and cell buffy coats are gently removed. As will be mentioned in Sec. 2.4, our model database consists two sample groups: (1) samples that are designed with different measurement conditions: flow rate, temperature, and flowcell pathlength with six different glucose levels and three Hct levels; and (2) saccharide containing samples. For the first group, red blood cells (RBC) are reconstituted with plasma to generate different Hct levels. A wide range of samples are created from three Hct levels and six glucose stock concentrations. Each blood sample is spiked with glucose concentration at least ten minutes before the sampling process and that the sample is gently mixed during that time. A small blood sample is also kept for Hct and glucose readings. For the second group, RBCs are then reconstituted with plasma to create a mid-range Hct level. High concentration glucose stock solution prepared with saline is used to spike the blood to three different glucose levels. Interference solutions are also prepared with saline and at ten times the tested concentration. Saccharide interferences are mixed at least 12 h before testing time to ensure the anomeric stability of solutions. These concentrated interferences are then added to blood at a 1:10 ratio to yield the final testing concentration and at least 10 min before the sampling process. Samples for the prediction set are prepared as follows: RBCs are reconstituted with plasma to create a mid-range Hct level. High concentration glucose stock solution prepared with saline is used to spike the blood. Saccharide interferences are mixed at least 12 h before testing time to ensure the stability of solutions. These concentrated interferences are then added to blood at a 1:10 ratio to yield the final testing concentration at least 10 min before the sampling process.

2.3 *Measurements*

FT-NIRS measurements were performed on whole blood samples obtained from 14 anonymous patients. Spectra were collected in transmission mode in the spectral region from 4000 to 8000 cm^{-1} from two FT-NIR systems (Nos. 7 & 8). Symmetrical interferograms that contained 2048 point were measured at 32 cm^{-1} resolution at full throughput. Background spectra of Saline (NaCl 0.9%) were collected before and after blood sample measurement for 30 s to account for variation in instrument noise and drift profiles. On the other hand, blood measurements were obtained for 60 s. Each background and blood measurement is an average of ~230 and ~460 spectra, respectively. Reference measurements were made by two bench whole-blood glucose analyzers, YSI 2300, which has an accuracy of ± 3 mg/dL; instrument A versus instrument B (1 sigma). Glucose samples were in the concentration range of 30–500 mg/dL with variable Hct levels ranging from 24 to 48 vol.%. For drug measurements to be included in the calibration and validation model the NIR interference is measured by spiking a control blood sample with an interferent and measuring the NIR glucose for the spiked sample versus an untreated control sample (the control sample has an identical volume of saline without the interferent). In this manner, interferent spiked and control samples are serially measured following CLSI guidelines (EP7-A2, Interference Testing).

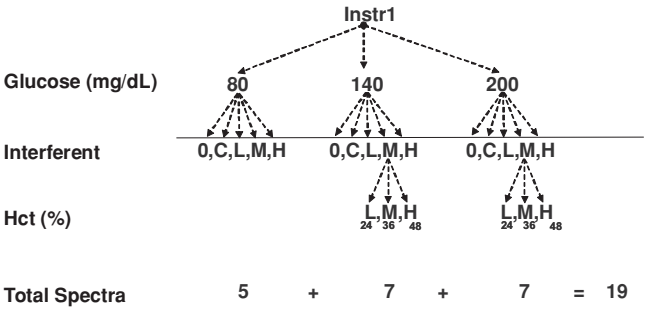

Fig. 2 Simple factorial design samples file to accommodate for single inteferent for each instrument used in this study. L- low, M- mid, H-high.

2.4 *Calibration Model*

The goal during NIR calibration is to increase analytical specificity or selectivity for glucose and decrease the effects of interferents. For that, a PLS1 model was used to develop a multivariate calibration model for predicting glucose concentration from the NIR spectra.[14] Spectra here refer to the absorbance data given by the modified Beer–Lambert law[15]

$$\mu_a = \log_{10}\left(\frac{I_{bck}}{I_{bld}}\right), \tag{1}$$

where μ_a is the absorption coefficient, I_{bck} is the background intensity, and I_{bld} is the light intensity from the blood.

Calibrations for glucose must be designed such that they are sensitive to changes in glucose concentration but are insensitive to interferent chemicals. A method for making calibrations more selective to the analyte of interest and less selective toward an interferent includes the use of "interferent compensation." This is accomplished by including low (nonzero), medium, and high concentration samples into the initial calibration and testing the sensitivity of the calibration to glucose and to the interferent following the incorporation of such samples into the initial calibration. A standard factorial design for including such samples is depicted in Fig. 2. This is implemented by taking the same basic blood sample with three different Hct levels (24, 36, and 48 vol.%) and spiking it to three levels of glucose (80, 140, and 200 mg/dL), and three levels of interferent (low, mid, and high expected physiological concentration). Table 1 summarizes these ranges of expected concentration for each

Table 1 Three level of interferent concentration used in this work. To convert mg glucose/dL to mmol/L, divide by 18.015

Interferent Type	Low (mg/dL)	Mid (mg/dL)	High (mg/dL)
Fructose	6	12	18
Galactose	20	40	60
Mannitol	200	400	600
Xylose	10	15	20
Dextran	1000	2000	3000
Maltose	60	120	180

inteferent. These intervals of values are near those commonly used in ICU and in OR. In addition, a combination of spectra from sample types with "real-world" effects (instrument type, sample temperature, flow rate, and flowcell pathlength) was added to the calibration model. Hence, our calibration data is formulated from a mixture of two groups of samples. The first group ($N = 1007$) is the real-world samples while the second ($N = 361$) contains the saccharide samples at constant: flow rate (0.5 ml/min), temperature (25°C) and flowcell pathlength (1 mm) state.

Outlier detection based on both Mahalanobis distance (MD) and spectral F-ratio (SFR) metrics were applied to ensure the quality of the data used to construct the calibration model. A criterion of $\mu \pm 3\sigma$ was used as an outlier screening for each metric. μ and σ represents the mean and the standard deviation receptively of the MD (or SFR). Samples that exhibit MD and SFR above this criterion were considered an outlier and removed from the calibration model. OSC was applied for preprocessing of the NIR spectra before being used in the PLS model. As stated in Sec. 1, the main goal of OSC is to determine and remove from the spectral data, $\boldsymbol{X}$, the part of information that is not correlated with the concentration, $\boldsymbol{Y}$, within a limited number of orthogonal scores (t) and loadings (p). Filtered data are obtained after iterative removal of the orthogonal components as follows:

$$X_{OSC} = X - \sum_{i=1}^{n} t_i \cdot p_i^T, \tag{2}$$

where n is the number of times that the treatment is applied. Usually, one factor is commonly used in OSC correction; the second treatment on the corrected $\boldsymbol{X}$ data can remove useful information reducing the predictive analytical ability.[16]

After outlier screening and OSC treatment, a PLS calibration matrix is formed. A leave-one-out method of cross-validation was performed on the calibration data set to determine the optimal number of factors (i.e., latent variables). The PLS model size was chosen as the number of factors resulting in the first minima of the standard error of cross-validation (SECV). Common calibration statistics such as SECV, mean relative error, coefficient of determination (R^2), etc. were computed to assess the fitting ability of the model. Once a model has been built, it can be used to predict the concentration of the unknown samples.

2.5 *Validation Model*

Validation data sets were composed of saccharide samples similar to the data included in the calibration model. These data sets differ from those in the calibration in their concentration level (Table 1, third column) and in the time when they were measured. The spectral data matrix, $\boldsymbol{X_{val}}$, was constructed by serially measuring new spectra of different interferences and control samples according to the following manner: Control, Interfernt1, Control, Interfernt2, Control, ..., Interferent n, etc. such that each block-run consists of ten interferent and ten control samples. The interferent treated test samples are immediately measured following the control samples and include an identical dilution volume of saline only as an added volume. $\boldsymbol{X_{val}}$ was then subtracted from the scores and loading vector obtained from the calibration model;

$$\tilde{X}_{Val} = X_{Val} - t \cdot p'_{Cal}, \tag{3}$$

where t is a new scores vector given by $t = X_{Val} \cdot \hat{b}_{Cal} \cdot (p'_{Cal} \cdot \hat{b})^{-1}$ and p_{Cal} is the loading vector determined by the OSC in the calibration model [see Eq. (2)]. The prime ($'$) represents the transpose matrix operation. For the validation procedure, $\boldsymbol{X}_{val}$ is multiplied by the prediction vector $\hat{b}_{Cal}$

$$Y_{Val} = \hat{b}_{Cal} \cdot \tilde{X}_{Val}. \tag{4}$$

2.6 *Computation and Software*

All computations were performed in Matlab software (Mathworks, Inc., R2008b) on an Intel Pentium (T4400) running at 2.2 GHz with 4GB memory. PLS program for calibration-prediction was obtained using PLS-Toolbox (Eigenvector Company, Ver. 2.1) and OSC m-file achieved from Ref. 17. Preprocessing algorithms were written in-house in Matlab language. During data processing the region of 4935–5300 cm^{-1}, representing the water band, was cut off (i.e., trimmed) in order to eliminate noise caused by high water absorption.

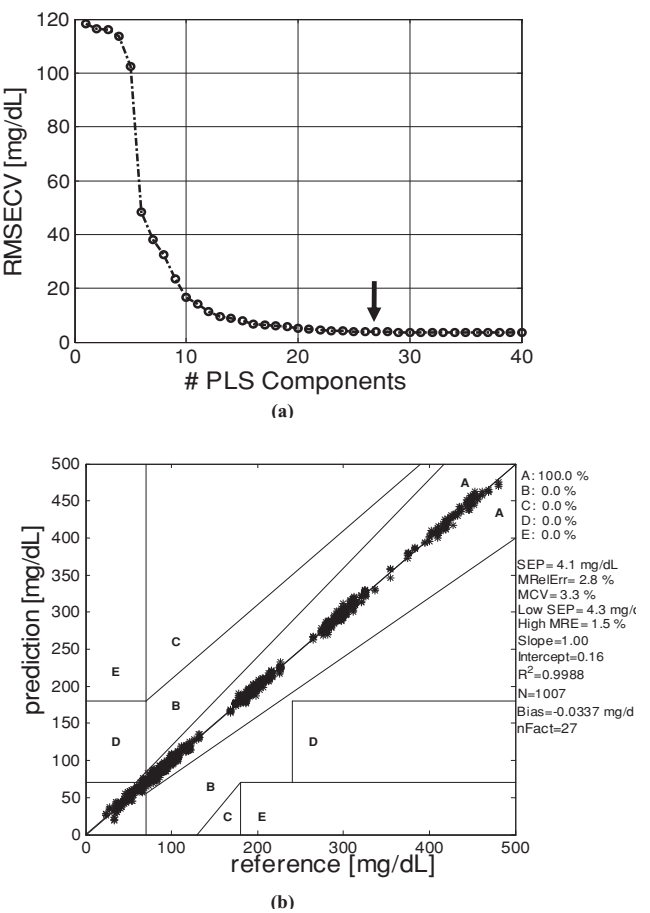

Fig. 3 (a) Plot of the root mean square of standard error of cross-validation (RMSECV) values versus the number of factors used to build the PLS. The arrow indicates the lower RMSECV values results in 27 factors. (b) Cross-validated PLS glucose prediction versus actual glucose concentration with Clark error grid. Cross-validation was performed by leaving one spectrum out of the calibration model at a time.

3 Results and Discussion

The aim of the first experiment was to investigate the effect of the saccharide interferences, on the prediction (validation) data sets. A PLS calibration was built with 1007 spectra from the real-world group as described in Sec. 2.4. The number of PLS factors used in the model and the cross-validation glucose prediction plot in the Clarke Error Grid Analysis (CEGA) format of these data sets are presented in Figs. 3(a) and 3(b), respectively. Usually, CEGA is used to quantify clinical accuracy of blood glucose measurement techniques in comparison to a reference value.[18] The grid consists of five zones *A–E* and provides an assessment of measurement errors and their respective clinical significance. For example, zone *A* is the region in which the NIR analytical values are within 20% of the reference values and indicates errors without serious clinical implications. As depicted, a linear correlation of $R^2 = 0.99$ between the NIR results and the YSI glucose concentrations, with SECV = 4.1 mg/dL is observed. These results, together with the fact that 100% of the prediction fall within zone *A* and zero% results on the other zones, confirm both the ability of PLS to calibrate models by using NIR spectra with real-world effects and the reliability of our FT-NIRS modality. Once the calibration is complete, the prediction data sets were build composed by six saccharide interferences: Dextran, Fructose, Galactose, Maltose, Mannitol, and Xylose. For interferent compensation, each interferent was spiked with different concentration levels and different glucose and Hct levels as per a factorial design depicted in Fig. 2; Table 2 shows an example for the Xylose experiment. The NIR predictions are reported under two basic conditions: 1. extrapolation testing without calibration interferent accommodation (compensation) of the test interferent compounds, where the calibration model predicts outside of its calibration space, and 2. interpolation with calibration interferent accommodation (compensation) of the test interferent compounds (i.e., including the extremes within the model), where the model predicts within its calibration space. Figure 4 together with Table 3 presents the results of the prediction in terms of maximum interference effect (MIE). MIE is expressed by

$$MIE = |NIR - YSI| + 1.96 \times \left(\frac{SEP}{\sqrt{n}}\right), \tag{5}$$

where NIR and YSI are the average value from the NIR prediction and YSI readings, respectively. SEP is the standard error of prediction given by

$$SEP = \sqrt{\frac{\sum(\hat{y} - y)^2}{N_p}}, \tag{6}$$

Table 2 Example of Xylose sequence measurements. Total sample measurements are equal to 26. Discontinuity in Sample ID results from the measurement of other inteferent according to CLSI Guidelines.

Sample ID	Hct (%)	Glucose (mg/dL)	Xylose Concentration (mg/dL)	System #
1000766	36	80	10	7 & 8
1000768	36	80	15	7 & 8
1000770	36	80	20	7 & 8
1000774	36	140	10	7 & 8
1000776	24	140	15	7 & 8
1000778	36	140	15	7 & 8
1000780	48	140	15	7 & 8
1000778	36	140	20	7 & 8
1000786	36	200	10	7 & 8
1000788	24	200	15	7 & 8
1000790	36	200	15	7 & 8
1000792	48	200	15	7 & 8
1000794	36	200	20	7 & 8

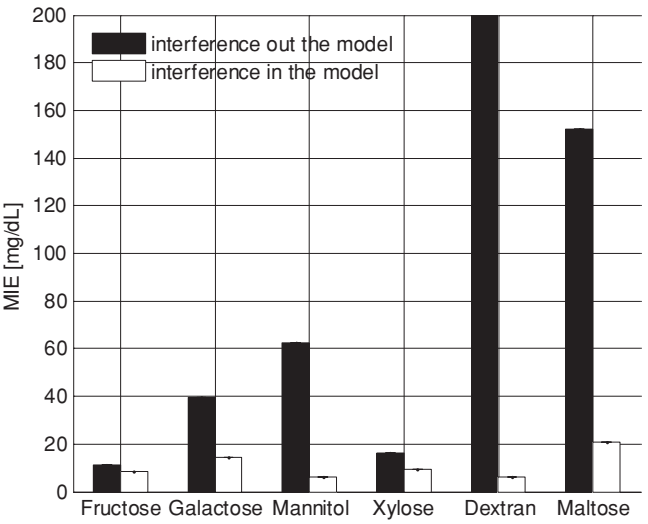

Fig. 4 Bar graph represents the difference in the MIE values when interferents *out* (black) or *in* (white) the calibration model.

Table 3 Comparison of the prediction results of Maximum Interference Effect (MIE) for six saccharide interferences when exclude and include in the calibration model.

Interferent Name	Interferent exclude Calibration (mg/dL)	Interferent include Calibration (mg/dL)
Fructose	11.1	8.6
Galactose	39.7	14.5
Mannitol	62.4	6.2
Xylose	16.4	9.5
Dextran	2599.6	6.2
Maltose	152.2	20.8

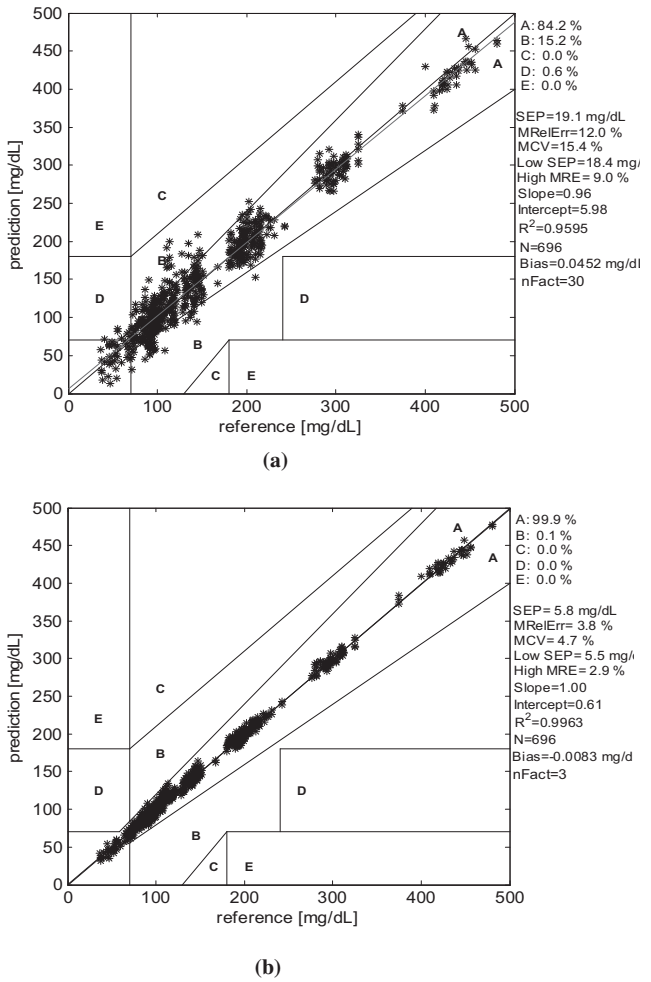

Fig. 5 Cross-validated results of glucose prediction versus reference values shown on Clark error grid before (a) and after (b) using OSC.

where $\hat{y}$ is the predicted glucose value, y is the known glucose value, and Np is the number of spectra used in the prediction sets. n in Eq. (5) represents the number of spectra used for each interferent and was equal to $n = 26$ (see Table 2). The differences between the MIE values are clearly shown in Fig. 4 and indicate, as expected, the influence of the interferent when excluded/included for both the calibration and validation models.

Before assessing the feasibility of *sb*OSC, a new experiment (experiment #2) was conducted in order to validate the efficacy of the standard OSC on interferent containing sample prediction. In this experiment a PLS calibration was constructed with 696 spectra obtained from a combination of a third set of real-world random samples ($N = 335$) and saccharide interferences ($Ns = 361$) having different concentrations. The performance of the calibration model before and after the use of OSC is shown in Figs. 5(a) and 5(b), respectively. Inspection of the correlation plots in Fig. 5(b) in comparison with Fig. 5(a) reveals that with OSC processing the prediction results are considerably concentrated along the unity line with $R^2 = 0.99$ and a ~70% decrease in SECV (19.1 mg/dL versus 5.8 mg/dL). In addition, Fig. 4(b) shows that a high percentage of the NIR predicted data points fall within the zones *A* and *B* of the Clarke grid; 99.9% and 0.1% of all NIR predictions fall in the *A* and *B* zones, respectively.

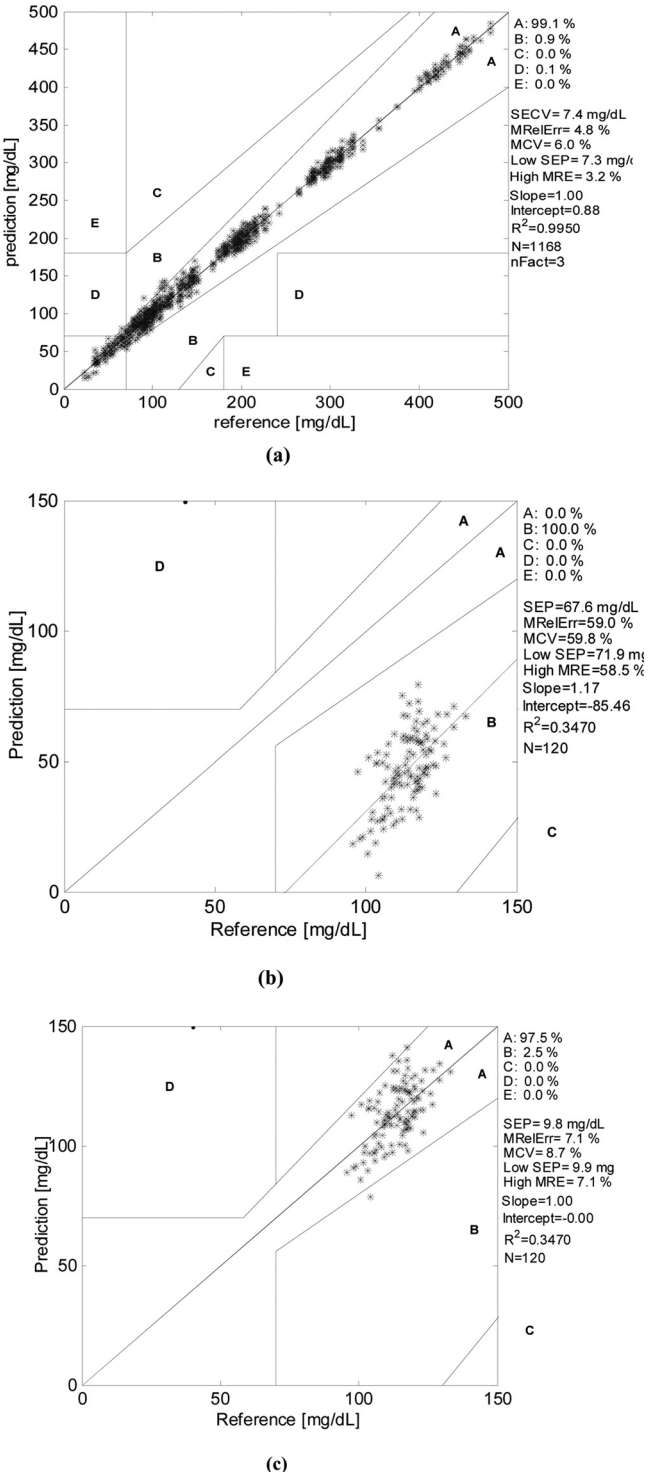

Fig. 6 Representative cross-validation performance (a) and predicted glucose concentration for a validation set (b) versus actual values observed during modeling. In (c), the slope and bias correction were applied to the validation set, noting the prediction performance is on samples that did not participate in the calibration modeling process.

On the contrary, without using OSC, 84.2%, 15.2%, and 0.6% of the predictions fall in the *A*, *B*, and *D* zones, respectively, resulting in a much higher error expressed as SECV.

The next experiment's (experiment #3) purpose was to establish a statistical method for computing the calibration slope (m) and bias (i, intercept) used later during the *sb*OSC procedure.

Table 4 Comparison of calibration and validation performance between *sb*OSC to several background correction methods. Validation results are present as the Maximum Interference Effect (MIE) in mg/dL. The validation data sets are saccharide interferences non-included in the calibration model.

	Calibration set			Validation set					
Calibration Approach	No. of PLS components	SECV (mg/dL)	R^2	Dextran (mg/dL)	Fructose (mg/dL)	Galactose (mg/dL)	Maltose (mg/dL)	Mannitol (mg/dL)	Xylose (mg/dL)
Factorial	33	21.9	0.934	27.8	18.3	53.9	66.3	47.4	41.7
2nd SG	30	21.7	0.933	34.6	22.7	61.6	72.0	50.3	44.9
WT	30	20.0	0.946	21.8	19.8	57.2	60.7	54.0	50.4
SLSN	29	22.5	0.927	33.1	18.6	52.8	70.2	20.0	48.4
DOSC	1	11.7	0.982	27.2	14.7	53	63.8	18	44.9
OSC	3	7.4	0.996	12	2.2	13.1	13.9	9.2	12.5
*sb*OSC	3	7.4	0.996	10.9	2	12	12.6	8.3	11.3
Percent improvement between *sbOSC* to Factorial approach				61%	89%	78%	81%	82%	73%

Table legend: 2nd SG - second derivative Savitsky-Golay, WT - Wavelet Transform, SLSN - sample selection, DOSC - direct orthogonal signal correction, OSC - orthogonal signal correction, *sb*OSC - slope and bias orthogonal signal correction

Eighty percent of the data set of random real-world samples ($N = 807$) were combined together with saccharide interferences ($Ns = 361$) in order to build an NIR calibration model. OSC was applied for preprocessing of the NIR spectra of these mixed samples ($N_T = 1168$) before being used in the calibration modeling step. The validation data sets were composed of the same saccharide type molecules, however, as previously mentioned, with high physiological concentration levels (Table 1, third column). In addition, the spectra of these validation samples were collected on the same two FT-NIRS instruments 35 days after the samples used for calibration. A total of 100 calibration models were developed by selecting different random samples for calibration and validation in order to determine the distribution for the slope and bias. For each set of experiments m and i metrics were computed according to the following expressions:

$$m = \frac{n \cdot \sum_{i=1}^{n} (\hat{y}_i \cdot y_i) - \sum_{i=1}^{n} \hat{y}_i \cdot \sum_{i=1}^{n} y_i}{n \cdot \sum_{i=1}^{n} \left(\hat{y}_i^2\right) - \sum_{i=1}^{n} (\hat{y}_i)^2},$$

$$i = \frac{\sum_{i=1}^{n} \hat{y}_i^2 \cdot \sum_{i=1}^{n} y_i - \sum_{i=1}^{n} \hat{y}_i \cdot \sum_{i=1}^{n} (\hat{y}_i \cdot y_i)}{n \cdot \sum_{i=1}^{n} \left(\hat{y}_i^2\right) - \sum_{i=1}^{n} (\hat{y}_i)^2}, \quad (7)$$

where $\hat{y}_i$ is a predicted value of a sample i, y_i is the known (reference) value for that particular sample, and n is the total number of samples. The average $\pm$ standard deviation of the slope and bias were found to be $\overline{m} = 1.07 \pm 0.032$, and $\overline{i} = -71 \pm 3.5$, respectively. These values will be used as correction metrics for the next experiment. One representative cross-validation and prediction plot before and after slope and bias correction are presented in Figs. 6(a)–6(c), respectively. Please note that the slope and bias in Fig. 6(c) are equal to 1 and 0, respectively, as a result of the correction. This correction was achieved by the following;

$$\hat{y}_{new} = \frac{\hat{y}_{old} - \overline{i}}{\overline{m}}, \quad (8)$$

where $\hat{y}_{old}$ and $\hat{y}_{new}$ are the predicted glucose value before and after the slope and bias correction, respectively. In addition, among the 120 validation data, 97.5% were in the A zone, 2.5% in B zone, and 0% were in C, D, and E zones. Thus, all NIR analytical values fell in areas where the error had no negative impact on resulting therapeutic decisions, thus no values fell where inaccurate values might cause clinically significant errors.

After identifying the slope and bias factors, a random data set of entire real-world samples ($N = 200$) were combined together with the saccharide interference samples ($N = 361$) to construct the PLS model for the calibration. Prediction data sets, not included in the calibration model, were employed as an independent test set. Therefore, our validation process is obtained on "blind" saccharide interferents samples. In addition the prediction equation from Eq. (4), was modified accordingly by

$$\tilde{Y}_{Val} = \frac{Y_{Val} - \overline{i}}{\overline{m}}, \quad (9)$$

where $\overline{i}$ and $\overline{m}$ are the average slope and bias reported above. After Eq. (9) was automatically applied on the validation saccharide interferent sets, MIE values were calculated based on Eq. (5). Since in this experiment the validation data measurements are following EP7-A2 protocol, in which the control and the interferent spectra are consecutively measured in time (control, Interfernt1, control, Interfernt2, control,..., etc.), Eq. (9) was separately applied for both the interferent and control samples and the final value was determined by subtraction of the two,

$$\tilde{Y}_{Val_{final}} = \tilde{Y}_{Val_{Intr}} - \tilde{Y}_{Val_{Cntrl}}. \quad (10)$$

Table 5 Comparison of calibration and validation performance of *sb*OSC when Dextran excluded during modeling. Validation results are present as the Maximum Interference Effect (MIE) in mg/dL.

	Calibration set			Validation set					
Calibration Approach	No. of PLS components	SECV (mg/dL)	R^2	Dextran (mg/dL)	Fructose (mg/dL)	Galactose (mg/dL)	Maltose (mg/dL)	Mannitol (mg/dL)	Xylose (mg/dL)
Factorial	30	20.1	0.939	-	15.5	52.4	66.4	19.2	41.2
OSC	3	5.4	0.996	-	1.5	11.7	12.1	5.3	10.7
*sb*OSC	3	5.4	0.996	-	0.5	10.6	11	4.7	9.8

In the next experiment (experiment #4), following Sec. 2.5, the purpose was to evaluate the bias and slope approach as *sb*OSC in comparison to other basic preprocessing approaches. After the spectral data matrix, $\boldsymbol{X}$, of the combined samples of real-world samples ($N = 1007$) with saccharide samples ($N = 361$) was corrected with a different correction technique, a PLS model was built and prediction on blind saccharide interferents ($N = 120$) was obtained. The MIE results are summarized in Table 4. The factorial approach appearing in Table 4 represents the data set without using any preprocessing correction approach, only the factorial design for data set construction. The MIE results for this category show that the prediction of the PLS is poor and should be improved. Next, the Savitzky–Golay method with nine points of smoothing and second derivative differentiation was performed. As observed, no improvement was obtained. Although, not shown in this paper, we used different smoothing points, different fitting polynomial, and also first derivative approaches to help reduce the MIE values, yet no dramatic prediction improvements were observed. Biorthogonal wavelet transform (WT) and sample selection (SLSN) algorithm was used next, unfortunately without improvement. The MIE result of the SLSN method to Mannitol is better from the previous correction method, but the overall performance for the other interferents is still not clinically acceptable. SLSN is an algorithm that subtracts unusual spectra from the others.[19] This kind of approach corrects the distribution of spectra used for calibration from normal to flat increasing the variability of the samples for calibration; it computes a data set with the largest concentration difference for chemical constituents and instrumental effects. Direct orthogonal signal correction (DOSC) was used next. Briefly, in DOSC instead of orthogonalizing X to Y using a regular PLS model, it uses the Moore–Penrose inverse calculation.[20] Use of DOSC yields dramatic changes of the calibration parameters, however, the results showed a reduction in MIE value only for Fructose and Mannitol for the validation sets. On the other hand, using OSC a distinct decrease in the validation performance of the MIE values occurs across the entire set of interferent. Finally, compared to OSC, *sb*OSC was able to further decrease the MIE values in validation analysis by an additional 10% for each interferent. For the reader's convenience, the bottom of Table 4 displays another Table line that summarizes the percent change (improvement) in the MIE value between *sb*OSC with that of the factorial approach. The results showed in Table 4 verified that OSC and *sb*OSC are greatly effective preprocessing approaches that enable the reduction of the influence of interferents on the accuracy of glucose measurements. In the next experiment (experiment #5), the Dextran, which is characterized with the highest concentration (i.e., 3000 mg/dL) as compared to the other saccharide interferents was removed from the calibration model. We hypothesize that this high interferent concentration of a glucose-like compound can affect the prediction accuracy of the NIR calibration model. The previous experiment was repeated again but now without using the Dextran. Results are presented in Table 5. In comparison to Table 4, MIE parameter improvements of 15% and 60% for Fructose and Mannitol, respectively, is observed when the Dextran is removed. However, the overall performance of the other interferents is not significantly changed. By using OSC, MIE values were improved by 32%, 11%, 13%, 42%, and 14% for Fructose, Galactose, Maltose, Mannitol, and Xylose, respectively, in comparison to previous results (Table 4, OSC data). With *sb*OSC, the MIE values were improved by 75%, 12%, 13%, 43%, and 13% for Fructose, Galactose, Maltose, Mannitol, and Xylose, respectively, in comparison to previous results (Table 4, *sb*OSC data). These results confirm our hypothesis about the removal of Dextran at high relative concentration.

4 Conclusions

There are medicines that can cause hypoglycemia (low blood sugar) or hyperglycemia (high blood sugar) in diabetic and nondiabetic patients. These drugs have a possible effect to interfere with NIR glucose measurements. In this paper, a method for determination of glucose concentrations in blood in presence of saccharide interferences using FT-NIRS and *sb*OSC as a pretreatment method was demonstrated. *sb*OSC is based on the traditional OSC platform but in addition uses a universal slope and bias correction on the prediction sets. The slope and bias were computed during calibration using 100 different calibration models and are used later for the validation prediction and routine analysis. A clear advantage of OSC and *sb*OSC presented in MIE value performance is observed in comparison to other basic preprocessing spectral correction techniques (Table 4). The novelty of this work is our ability to directly quantify glucose value in the presence of saccharide interferences in NIR region using FTS, and the ability of the *sb*OSC approach to further decrease the MIE values by an additional 10% for each interferent over OSC-PLS. To the best of our knowledge, no previous report of such a study and calibration development has been previously described. The overall results presented in this study

clearly show the potential and versatility of our methodology, which could be applied for blood glucose assay in ICU and OR rooms.

References

1. M. B. Davidson, *Davidson's Diabetes Mellitus: Diagnosis and Treatment*, 5th ed., Saunders, Philadelpia (2003).
2. O. S. Khalil, "Non-invasive glucose measurement technologies: An update from 1999 to the dawn of the new millennium," *Diabetes. Technol. Ther.* **6**, 660 (2004).
3. K. J. Pezzaniti, T.-W. Jeng, L. McDowell, and G. Oosta, "Preliminary investigation of near-infrared spectroscopic measurements of urea, creatinine, glucose, protein, and ketone in urine," *Clin. Biochem.* **34**, 239 (2001).
4. M. A. Arnold and G. W. Small, "Noninvasive glucose sensing," *Anal. Chem.* **77**, 5429 (2005).
5. J. T. Olsberg, M. A. Arnold, C. Mermelstein, J. Schmitz, and J. Wagner, "Tunable laser diode system for noninvasive blood glucose measurements,"*Appl. Spectr.* **59**, 1480 (2005).
6. J. T. Olesberg, L. Liu, V. V. Zee, and M. A. Arnold, "*In vivo* near-infrared spectroscopy of rat skin tissue with varying blood glucose levels," *Anal. Chem.* **78**, 215 (2006).
7. K. Maruo, T. Oota, M. Tsurugi, T. Nakagawa, H. Arimoto, M. Tamura, Y. Ozaki, and Y. Yamada, "New methodology to obtain a calibration model for noninvasive near-infrared blood glucose monitoring," *Appl. Spectr.* **60**, 441 (2006).
8. V. R. Kondepati and H. M. Heise, "Recent progress in analytical instrumentation for glycemic control in diabetic and critically ill patients," *Anal. Bioanal. Chem.* **388**, 545 (2007).
9. Z. Tang, X. Du, R. F. Louie, and G. J. Kost, "Effects of drugs on glucose measurements with handheld glucose meters and a portable glucose analyzer," *Am. J. Clin. Pathol.* **113**, 75 (2000).
10. R. J. McEnroe, M. F. Burritt, D. M. Powers, D. W. Rheinheimer, and B. H. Wallace, *Interference Testing in Clinical Chemisrty; Approved Guidline – second ed.*, CLSI document EP7-A2 (Pennsylvania, 2005).
11. S. Wold, H. Antti, F. Lindgren, and J. Ohman, "Orthogonal signal correction of near-infrared spectra," *Chem. Intell. Lab. Syst.* **44**, 175 (1998).
12. H. Mark and J. Workman, *Chemometrics in Spectroscopy*, Elsevier, Amsterdam (2007).
13. A. P. Throne, *Spectrophysics*, 2nd ed., Chapman & Hall, London (1988).
14. P. Geladi and B. R. Kowalski, "Partial Least-Squares regression; a tutorial," *Anal. Chim. Acta* **185**, 1 (1986).
15. V. V. Tuchin, *Tissue Optics: Light Scattering Methods and Instruments for Medical Diagnosis*, 2nd ed., SPIE Press, Bellingham, Washington, (2007).
16. M. Blanco, J. Coello, I. Montoliu, and M. A. Rometo, "Orthogonal signal correction in near infrared calibration," *Anal. Chim. Acta.* **434**, 125 (2001).
17. http://www.eigenvector.com/MATLAB/PC_M_files/osccalc.m
18. W. L. Clarke, D. Cox, L. A. Gonder-Frederick, W. Carter, and S. L. Pohl, "Evaluating clinical accuracy of systems for self-monitoring of blood glucose," *Diabetes Care* **10**, 622 (1987).
19. D. E. Honigs, G. M. Hieftje, H. L. Mark, and T. B. Hirschfeld, "Unique-sample selection via near-infrared spectral substraction," *Appl. Spectrosc.* **57**, 2299 (1985).
20. J. W. Westerhuis, S. de-Jong, and A. K. Smilde, "Direct orthogonal signal correction," *Chemom. Intell. Lab. Syst.* **56**, 13 (2001).